The International Journal of Advanced Manufacturing Technology (2020) 106:4845–4857
https://doi.org/10.1007/s00170-020-04966-y

ORIGINAL ARTICLE

Attainment of high corner accuracy for thin-walled sharp-corner part by WEDM based on magnetic field-assisted method and parameter optimization

Hongzhi Yan[1] · Kabongo Djo Bakadiasa[1] · Zhi Chen[1] · Zhaojun Yan[1] · Hongbing Zhou[1] · Fenglin Han[1]

Received: 11 September 2019 / Accepted: 20 January 2020 / Published online: 28 January 2020

Abstract
The demand for thin-walled sharp-corner parts is constantly becoming higher in aerospace, precise instruments, and micro-electro-mechanical systems (MEMS). Nonetheless, the fabrication of thin-walled sharp-corner part is a challenging work because of its poor stiffness. Wire electrical discharge machining (WEDM) is an alternative method to machine low-stiffness part due to its non-contact material removal process. However, experimental data show that there exists an inevitable deformation in the corner area of thin-walled sharp-corner part. The goal of this paper is to achieve high corner accuracy for thin-walled sharp-corner part based on magnetic-assisted approach and parameter optimization. Firstly, a coupled magnetic-mechanical model is established to analyze the effect of the external magnetic field on the corner deformation. It can be found that the external magnetic field can effectively improve the magnetic field distribution and decrease the corner deformation. There is optimal external magnetic induction intensity between 0.2 and 0.3 T for smaller corner deformation. Then, the results of verification experiment indicate that the coupled magnetic-mechanical model is of high feasibility and reliability. In addition, a set of Taguchi experiment is implemented to investigate the influences of process parameters on the corner deformation. It can be obtained that corner deformation rises up with the increase of pulse on time and discharge peak current, and reduces along with pulse-off time. Furthermore, the optimal process parameter combination from the range analysis method can reduce corner deformation from 100 to 34.3 μm.

Keywords WEDM · Thin-walled sharp-corner part · Corner deformation · External magnetic field assisted

1 Introduction

Recently, due to the characteristics of low weight, saving material, compact structure, and good toughness, the thin-walled parts are increasingly used in the aerospace and precise instrument industry. Unfortunately, the fabrication of thin-walled part is a very challenging work due to its poor stiffness [1]. Specifically, it is difficult to fabricate thin-walled sharp-corner parts, using traditional machining methods, because of common machining deformation that reduces the form and dimensional accuracy of the parts [2]. Wire electrical discharge machining (WEDM) is a high-precision and non-contact machining method, which can process conductive materials of any hardness, without inducing cutting stress [3–5]. Thus, WEDM is an appropriate machining method for fabricating thin-walled sharp-corner part because of its specific material removing mechanism. However, according to our experimental data, there is an inevitable corner deformation during processing thin-walled sharp-corner part, and the direction of this corner deformation is closely related to the magnetism of the workpiece material. More specifically, as shown in Fig. 1, the direction of corner deformation of Q235 steel (magnetic materials) is opposite to that of 6061 Al alloy (non-magnetic material) under the same cutting path. The formation of this corner deformation may be caused by the induced magnetic field from the discharge current. Hence, this corner deformation is defined as electromagnetic deformation.

In addition, the WEDM process involves several physical fields, such as electric field, thermal field, electromagnetic field, flow field, and optics. The material removing process

✉ Zhi Chen
zhichen415@gmail.com

[1] State Key Laboratory of High Performance Complex Manufacturing, College of Mechanical and Electrical Engineering, Central South University, Changsha 410083, People's Republic of China

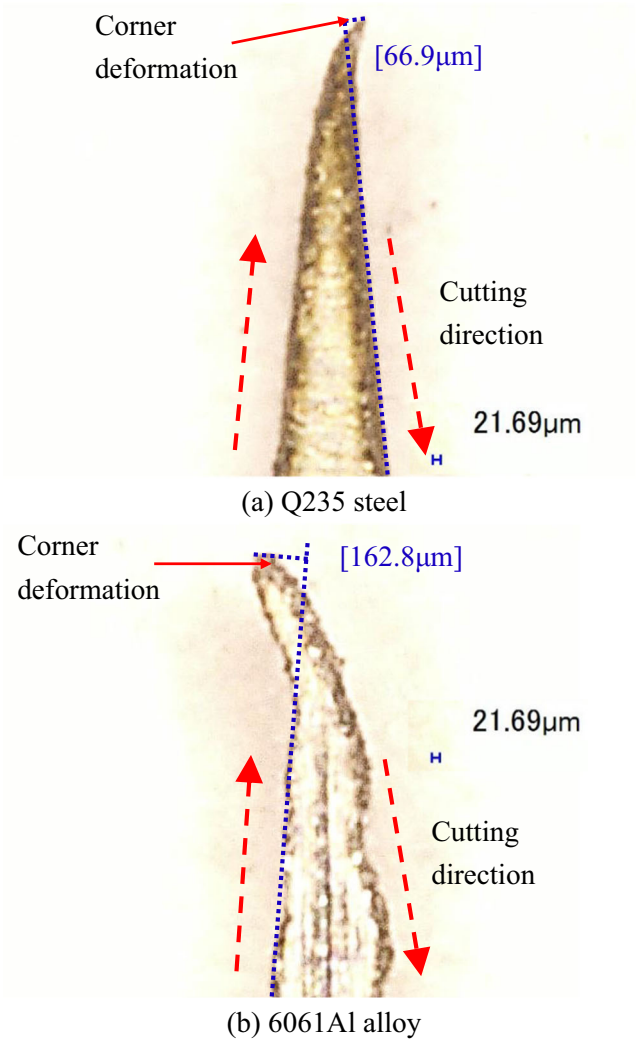

Fig. 1 The physical map of corner deformation of Q235 steel and 6061 Al alloy

of WEDM is widely considered as thermal removing. A part of workpiece material may be heated to austenitizing temperature. Then, the strength of this part of workpiece material is significantly decreased. Under the induced magnetic field, the material with lower strength will be resulted in more obvious sharp-corner deformation.

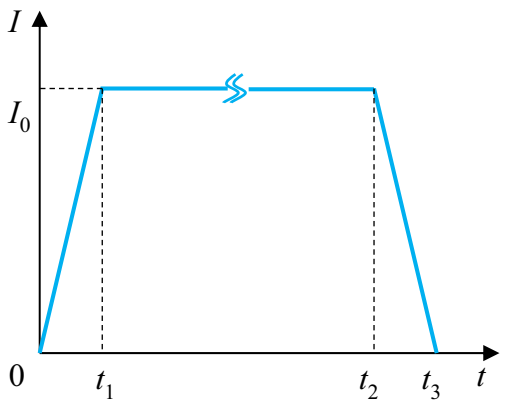

Fig. 2 The schematic diagram of the wave shape of the discharge current during single pulse discharge

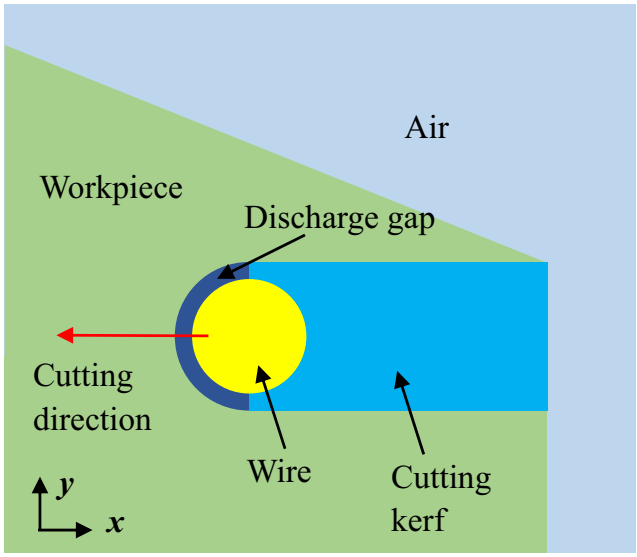

Fig. 3 The configuration of the coupled magnetic-mechanical model

Therefore, it can be said that the sharp-corner deformation is directly related to the induced magnetic field. Besides, the heating effect can promote the increase of the sharp-corner deformation.

As we know, cutting speed, surface quality, and geometrical accuracy are the three key indexes of WEDM characteristics. Thereinto, corner deformation is one of the main forms of workpiece geometrical accuracy. Besides, sharp corner is a common feature in the precision parts and components, such as precision mold, small module gear, clock, and robot. Investigating and reducing of the corner deformation of workpiece with sharp corner have good practical significance. For example, WEDM is a usual manufacturing method for small module gear in small batch and diversity product. Corner accuracy is the important technological index of small module gear which is a determining factor of transmission precision and service life. Hence, reducing the corner deformation of workpiece is helpful for increasing the usability of workpiece with sharp-corner and the promotion and application of WEDM in some precision manufacturing fields.

Table 1 The simulation parameters of the coupled magnetic-mechanical model

Parameters	Symbol	Value	Unit
Wire diameter	d_w	0.25	mm
Peak current	I_0	8	A
Rising time	t_1	2	μs
Dropping time	t_3–t_2	2	μs
Pulse on time	t_3	20	μs
Workpiece thickness	H	1	mm
Discharge gap width	d	30	μm

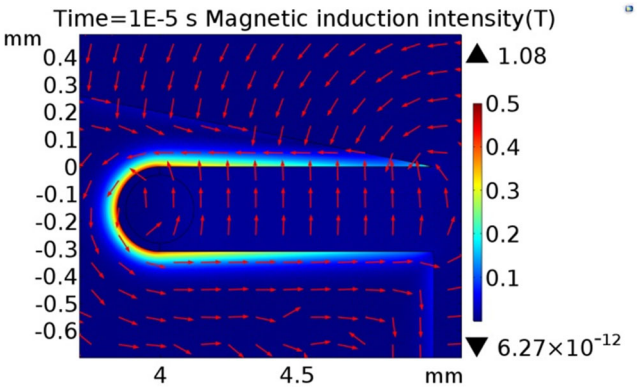

(a) Overall view

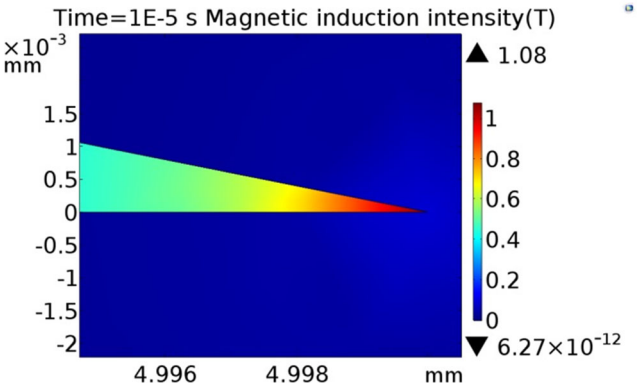

(b) Partial view of corner area

Fig. 4 The induced magnetic field distribution during single pulse discharge

1.1 Literature review

1.1.1 Corner accuracy

Han F et al. [6] presented a simulation system for predicting the corner error considering wire deflection and vibration in WEDM, and it was proved that this simulation system is of high feasibility and precision. Chen et al. [7] focused on investigating the causes of corner error during different cutting paths, and the method of parameter optimization was used to obtain high corner accuracy. Abyar et al. [8] built a mathematical model for investigating the inaccuracy at small arced corners due to wire deflection, and it was proved that the proposed mathematic model could be utilized to predict and compensate wire deflection during machining small arced corner process. Chen et al. [9] developed a wire deflection model for forecasting the corner error in WEDM, and a new wire electrode and cut-back method based on wire deflection model were proposed to reduce the corner error. Chen et al. [10] designed a constant wire tension control system to improve corner error due to wire deflection, and it was pointed out that this system could decrease corner error by 15–35%. Abovementioned studies about corner accuracy mainly concentrated on corner error due to wire deflection and vibration, and they were significant to reveal the formation mechanism and reduce corner error. However, very few researches focusing on corner accuracy of thin-walled sharp-corner part resulted from induced magnetic field exist.

1.1.2 Magnetic field distribution

A considerable number of researches about magnetic field distribution have been carried out. Tomura et al. [11] built a two-dimensional model to obtain the magnetic field distribution, based on Poisson's equation and taking into account electro-magnetic induction. It was noted that the force due to electromagnetic induction acting on the wire electrode was an attractive force when the workpiece material was magnetic. But, the force due to electromagnetic induction acting on the wire electrode was a repulsive force when the workpiece material was non-magnetic. Chen et al. [12] developed a three-

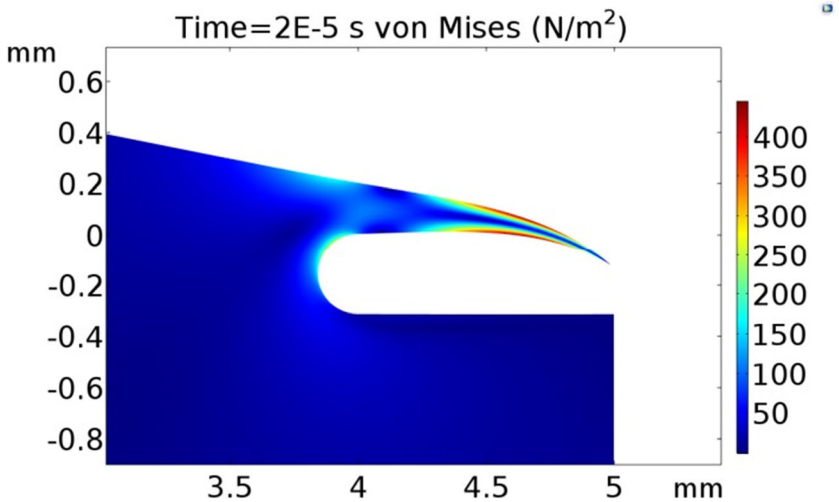

Fig. 5 The stress distribution and deformation of Q235 during single pulse discharge

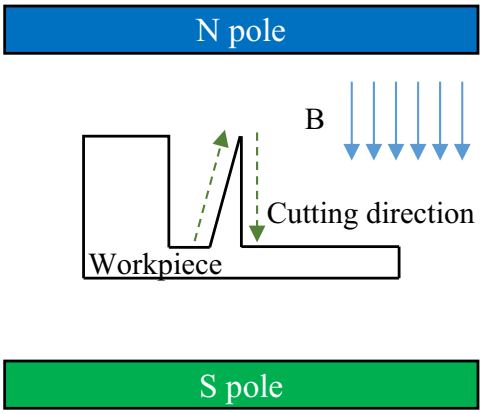

(a) Schematic map

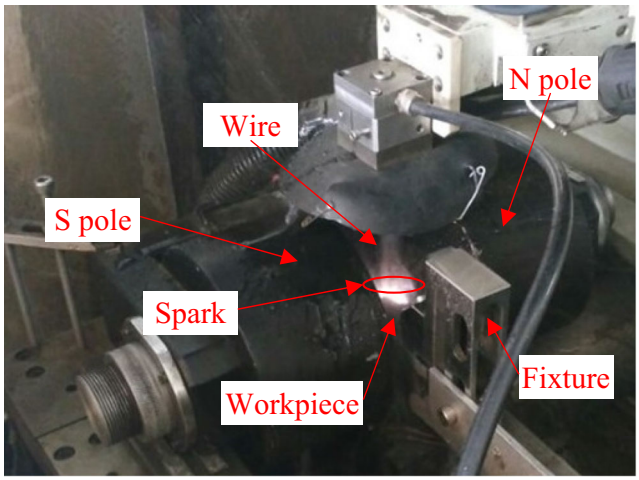

(b) Physical map

Fig. 6 The schematic and physical map of the external magnetic field-assisted WEDM

dimensional finite element model for analyzing the magnetic flux density distribution and the force due to electromagnetic induction exerted on the wire electrode. It was pointed out that this force due to electromagnetic induction acting on the wire electrode could be approximate to a periodic trapezoidal impulsive force. Nani et al. [13] presented an ultrasonic-assisted method to reduce the impact of the induced electro-magnetic field on the machining characteristics. Experimental results showed that this method could improve the dimensional accuracy and surface quality of the workpiece. Based on the abovementioned studies about magnetic field distribution, it can be found that the induced magnetic field caused by discharge current has a great effect on the machining

Table 2 The relationship between the external magnetic induction intensity and supplying current

Current (A)	4	4.5	5.5	7	9
B (T)	0.1	0.15	0.2	0.25	0.3

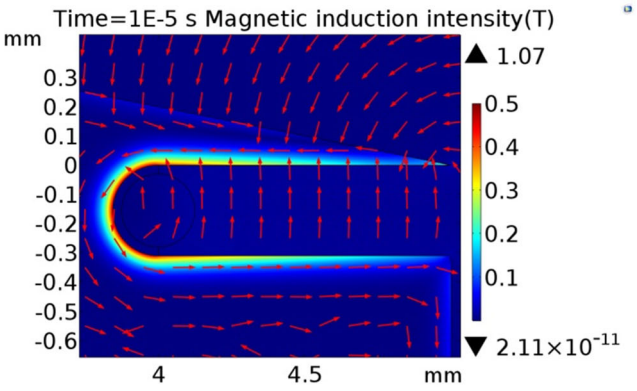

(a) Overall view

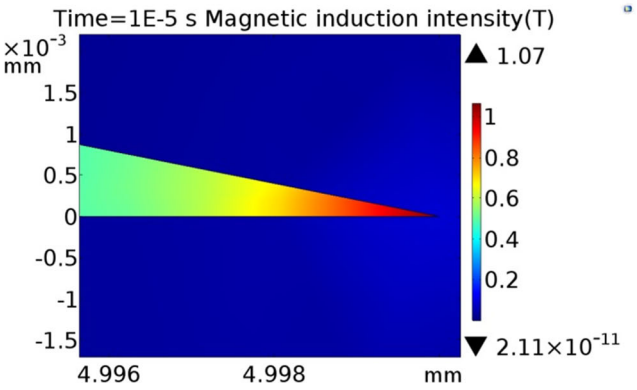

(b) Partial view of corner area

Fig. 7 The magnetic field distribution under 0.05 T magnetic field assisted

characteristics of WEDM, such as wire electrode vibration, workpiece geometric accuracy, and surface quality. Above previous researches contributed to understand how the induced magnetic field distribution affect the machining process of EDM/WEDM. However, very few researches about the influence of the induced magnetic field on the corner accuracy of thin-walled sharp-corner part exist.

1.1.3 Magnetic field-assisted method

Gholipoor et al. [14], Lin et al. [15–17], and Teimouri et al. [18] applied the method of magnetic field assisted to enhance the performance of EDM, and good improvements had been obtained in their researches, such as material removal rate and surface quality. Govindan et al. [19] pointed out that the magnetic field-assisted method could significantly restrain the expansion of the electron beam. Thus, the density of discharge energy could be raised so as to increase the volume of discharge crater in single pulse discharge process. Teimouri et al. [20, 21] came up with a method of rotational magnetic field assisted to enhance the debris expelling from the machining gap in EDM, and it was proved that the improvement of rotational magnetic field was more obvious than that of constant

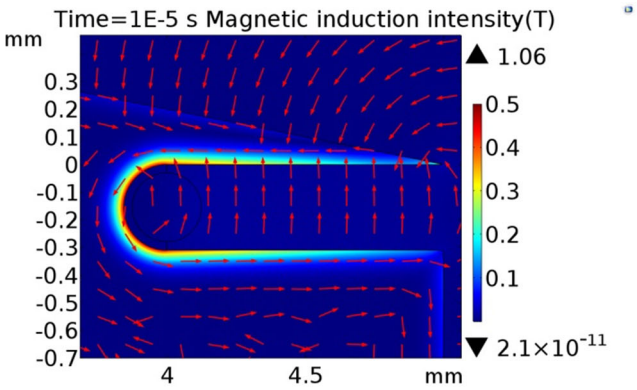

(a) Overall view

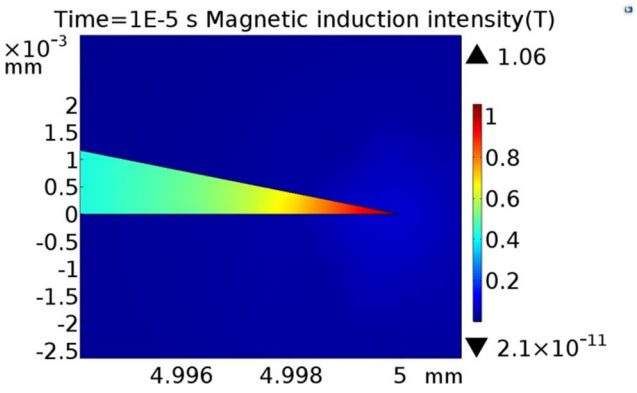

(b) Partial view of corner area

Fig. 8 The magnetic field distribution under 0.1 T magnetic field assisted

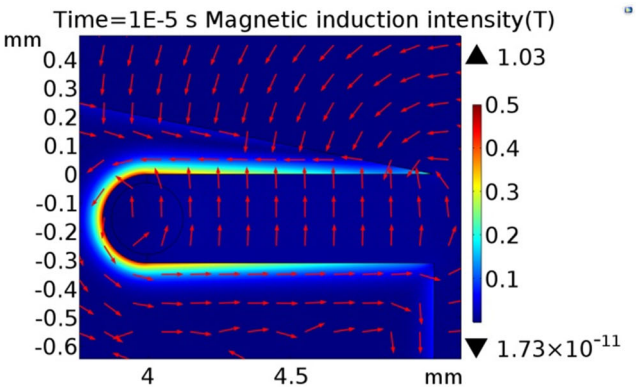

(a) Overall view

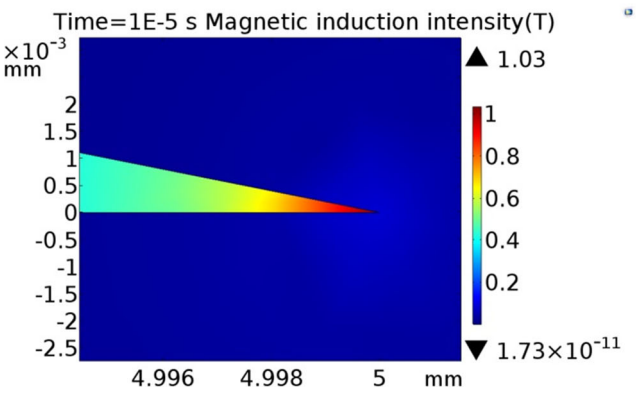

(b) Partial view of corner area

Fig. 9 The magnetic field distribution under 0.2 T magnetic field assisted

magnetic field. Heinz et al. [22] designed a new magnetic field device to assure that the Lorentz force, acting on debris, was vertical to the workpiece surface when the workpiece material was non-magnetic in EDM. Then, the material removal rate was increased by approximately 50% in single pulse discharge. Ming et al. [23] carried out a comparative study to evaluate the effect of magnetic field assisted on the energy efficiency and environmental impact. It was proved that the magnetic field-assisted method could increase energy utilization efficiency, material erosion efficiency, and material removal rate. Zhang et al. [24] adopted the magnetic field-assisted technology to reduce energy consumption and thermal deformation in WEDM. Zhang et al. [25] adopted the methods based on ultrasonic vibration and magnetic field to assist WEDM in improving its machining performance. It was concluded that this proposed hybrid approach could effectively increase the percentage of normal discharge state and improve the machining characteristics (including material removal rate, surface roughness, and surface crack density) when the process parameters were set within the appropriate range. Wang et al. [26] illustrated that the magnetic field-assisted method could make the distribution of discharge spark points more uniform in WEDM. Then, this method could reduce the probability of wire electrode breakage and improve machining characteristics. Chen et al. [27] proposed specific discharge energy and magnetic-assisted method for increasing the machining characteristics of WEDM; a good improvement for machining efficiency and surface quality had been obtained in their study. All the aforementioned studies prove that the magnetic field-assisted method could effectively improve the performance of EDM/WEDM. However, very few researches focusing on the effect of external magnetic field-assisted on corner deformation of thin-walled sharp-corner part exist.

1.2 Outline of our work

This paper aims to improve the corner accuracy of thin-walled sharp-corner part based on magnetic-assisted approach and parameter optimization. A coupled magnetic-mechanical model is established to clarify the function mechanism of the external magnetic field on the corner deformation. Besides, a confirmatory experimental study is carried out for verifying the theoretical influence rule of the external magnetic field on corner deformation. Moreover, a set of Taguchi experiment is implemented to analyze the effects of process parameters on the corner

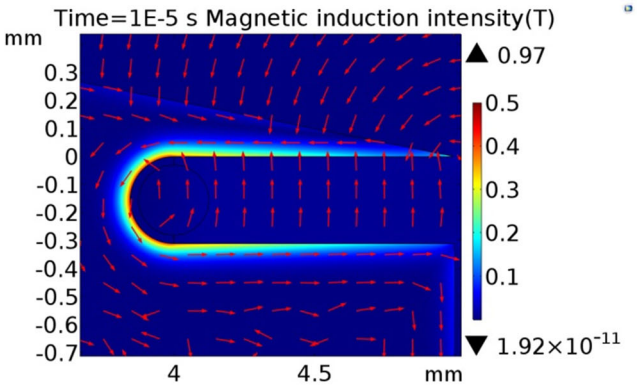

(a) Overall view

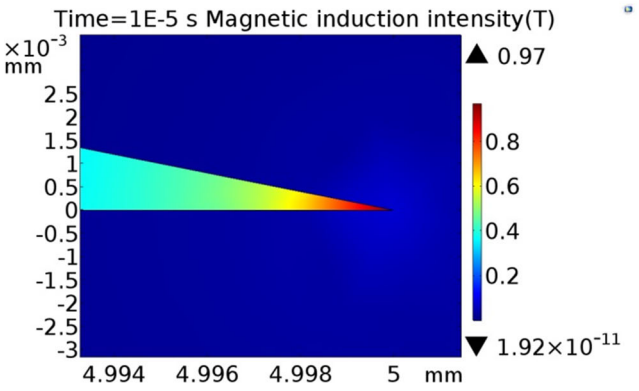

(b) Partial view of corner area

Fig. 10 The magnetic field distribution under 0.3 T magnetic field assisted

deformation. The numerical model of corner deformation is worked out to find the optimal process parameter combination for the minimum corner deformation.

2 The coupled magnetic-mechanical model

In this section, a coupled magnetic-mechanical model is built to describe how the external magnetic field affects the corner deformation. In addition, the influence trends of the external magnetic induction intensity on the magnetic field distribution and corner deformation are also investigated.

2.1 Without the external magnetic field assisted

The induced magnetic field caused by discharge current can be simplified as a two-dimensional problem because the workpiece thickness (1 mm) is negligible. Moreover, the magnetic field model follows the Poisson's equation taking into account electro-magnetic induction (as shown in Eq. (1)), and the mechanical model is according to solid mechanics theory.

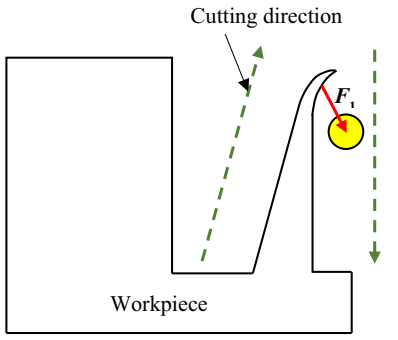

(a) Without the external magnetic field assisted

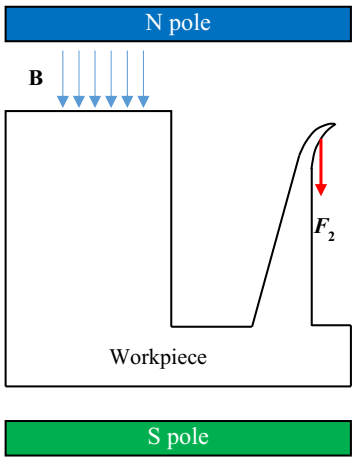

(b) Without discharge current

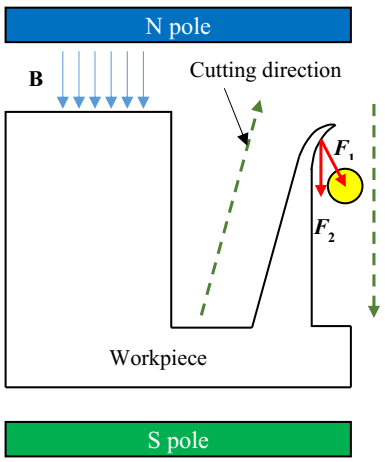

(c) With discharge current and the external magnetic field assisted

Fig. 11 The stress distribution and deformation under the external magnetic field during single pulse discharge

$$-J_0+\sigma\frac{\partial \mathbf{A}_z}{\partial t}+\sigma\frac{\partial \varphi}{\partial z}=\frac{\partial}{\partial x}\left(\frac{1}{\mu_r\mu_0}\frac{\partial \mathbf{A}_z}{\partial x}\right)+\frac{\partial}{\partial y}\left(\frac{1}{\mu_r\mu_0}\frac{\partial \mathbf{A}_z}{\partial y}\right) \quad (1)$$

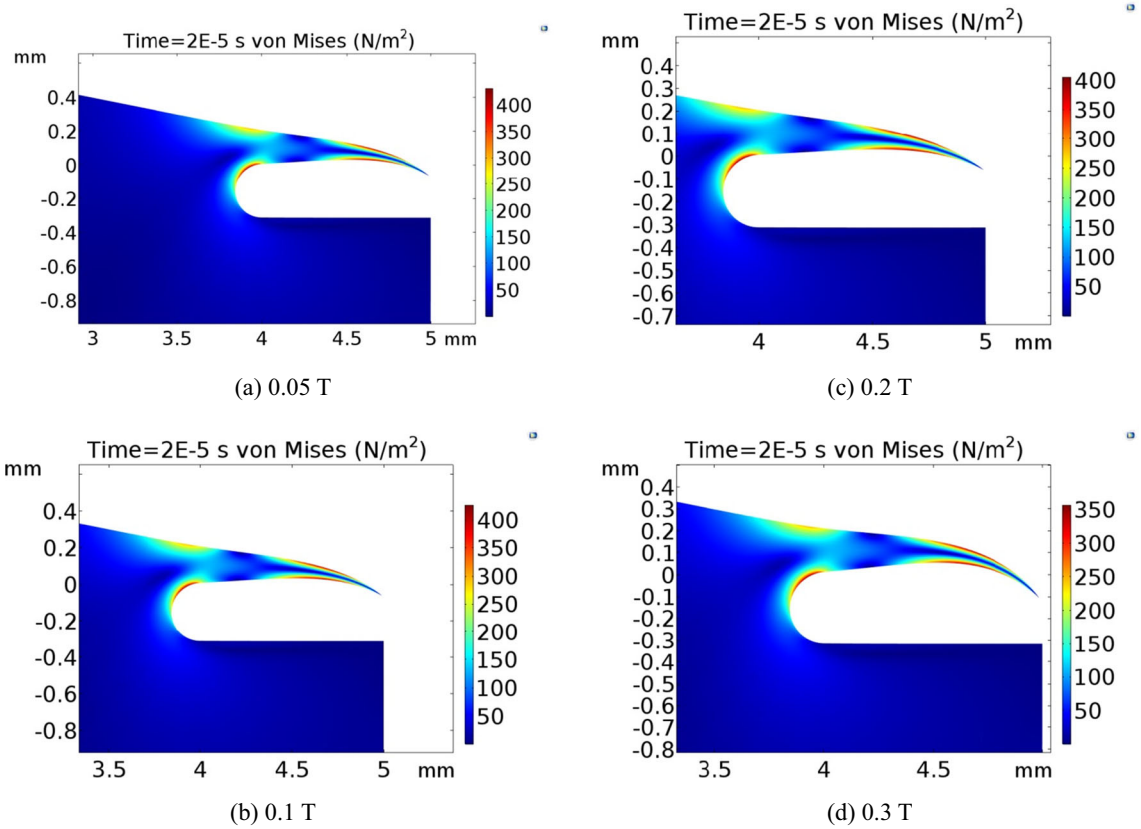

Fig. 12 The influence trend of magnetic induction intensity on the maximum corner deformation

where J_0 is the discharge current density which is equal to $I_{(t)}/\pi/r^2$, σ is the workpiece conductivity, φ is the induction electromotive force, μ_r is the relative magnetic permeability, μ_0 is the vacuum permeability, and A_z is the z-component of electro-magnetic vector potential. $\sigma(\partial A_z/\partial t+\partial\Phi/\partial z)$ is induced eddy current density due to the changing magnetic field.

Because the external magnetic field can only affect the induced magnetic field when the workpiece material is magnetic, Q235 steel is chosen as the workpiece material in the coupled magnetic-mechanical model due to its good magnetism.

Based on previous researches [11, 28, 29] and our own experimental experience, the wave shape of the discharge current, during single pulse discharge, is similar to trapezoid, as shown in Fig. 2. The discharge current rises up to a peak value (I_0) in a very short time (0–t_1), then remains stable for a certain period of time (t_1–t_2), and then drops rapidly to zero (t_2–t_3). In other words, the wave shape of the discharge current, during single pulse discharge, includes a constant current component and a variant current component. The changed current will result in electromagnetic induction phenomenon. In addition, according to the collecting experiment for the wave shape of the discharge current during single pulse discharge, the rising time and dropping time are about 2 μs when the pulse on time is 8–20 μs.

Figure 3 suggests the configuration of the coupled magnetic-mechanical model which consists of workpiece, wire electrode, discharge gap, cutting kerf, and air. Alone, the relative magnetic permeability of the workpiece is 400, while the others' are all zero. Besides, Table 1 represents the simulation parameters of the coupled magnetic-mechanical model. According to experimental measurement, the width of the cutting kerf is about 310 μm as the diameter of wire electrode is 250 μm. Then, the discharge gap is set as 30 μm in this coupled model.

Based on the above theoretical analysis, the coupled magnetic-mechanical model during single pulse discharge can be solved by the FEM numerical simulation software (COMSOL Multiphysics). Figure 4 illustrates the induced magnetic field distribution at the time point of 10 μs during single pulse discharge. It can be found that (1) the distribution of the induced magnetic field is not uniform, and the maximum induced magnetic induction intensity can be up to 1.08 T at the corner area; and (2) the direction of the magnetic force line in air region is anticlockwise. At the boundary area of the cutting kerf, the magnetic force line detoured around discharge gap rather than pass through it. In the cutting kerf region, the magnetic line force is approximately parallel to the y-axis and follows the positive direction. This fact is attributed to the electromagnetic induction phenomenon, as the relative magnetic permeability of the workpiece is much higher than those of other areas. Besides, based on the induced magnetic

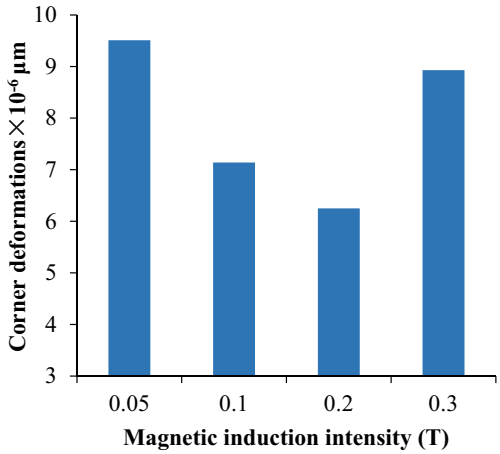

Fig. 13 The sharp-corner deformation under three machining conditions

field distribution, it is evident that the lower edge of the cutting kerf can be simplified to N pole, and the upper edge of the cutting kerf can be simplified to S pole. Then, the corner area is subject to the force whose direction is the same to *y*-axis negative direction.

Figure 5 exhibits the stress distribution and deformation of Q235 during single pulse discharge. The scale factor of deformation is 1.12×10^7. The maximum stress reaches 480 N/mm^2 at the corner point, and the maximum deformation is 1.07×10^{-5} μm. In other words, the corner deformation resulted by single pulse discharge is very small. As we know, the period of single discharge process is of the order of 0.1–1 μs, so the discharge sparks affect each other. Then, it is very difficult to predict the exact value of corner deformation by simulation. However, the direction of corner deformation is the same to that in experiment. That is to say, this coupled magnetic-mechanical model can qualitatively clarify the forming cause of corner deformation.

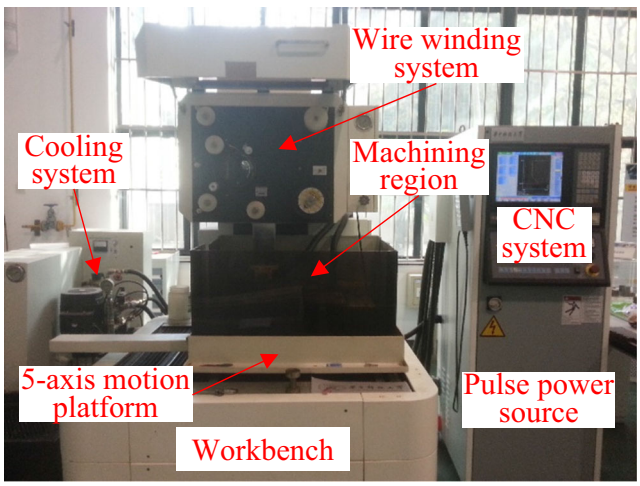

Fig. 14 The physical map of 5-axis low-speed wire electrical discharge machine tool

Table 3 The chemical compositions and ranges (wt%) of Q235

Element	C	Mn	Si	S	P	Fe
Ranges	≤ 0.17	0.35–0.80	≤ 0.35	≤ 0.40	≤ 0.35	Bal

2.2 With the external magnetic field assisted

Figure 6 suggests the schematic and physical map of the external magnetic field-assisted WEDM. Before we start this paper, we attempt to analyze the effect of the direction of the external magnetic field on the sharp-corner deformation. According to our experiment data, the external magnetic field can decrease the sharp-corner deformation only when the setting of the external magnetic field as Fig. 6. This device is composed of a DC electrical source, two solenoids, and iron cores. The principle of external magnetic field accords with the law of electromagnetic induction discovered by Faraday. The external magnetic induction intensity (B) between N pole and S pole is uniform because the two solenoids are the same and placed in parallel, and the supplying currents of two solenoids are in opposite directions. In addition, the external magnetic induction intensity is adjusted by supplying current, according to the relation shown in Table 2.

Based on the coupled magnetic-mechanical model, the magnetic field distribution and corner deformation under the external magnetic field assisted during single pulse discharge can be obtained through simulation method. Figures 7, 8, 9, and 10 depict the magnetic field distribution under the external magnetic field assisted during single pulse discharge. It can be observed that (1) the magnetic field distribution under the external magnetic field assisted is similar to that without the external magnetic-assisted approach. (2) Comparing with Fig. 4, it is evident that the external magnetic field can effectively improve the electromagnetic induction phenomenon caused by discharge current. (3) The improvement effect of the external magnetic field assisted has a positive relation with the

Table 4 The physical and mechanical properties of Q235

Parameters/properties	Unit	Value
Density	g/cm^3	7.85
Melting point	K	1766
Thermal conductivity	W/m/K	52
Specific heat capacity	J/kg/K	502
Electric conductivity	S/m	6.7×10^6
Relative magnetic permeability	1	400
Young modulus	GPa	200
Poisson's ratio	1	0.33
Yield strength	MPa	235
Tensile strength	MPa	460

Table 5 The design and results of the single factor experiment

No.	B (T)	t_{on} (μs)	t_{off} (μs)	I (A)	D (μm)
1	0	12	12	8	100.6
2	0.05	12	12	8	93.5
3	0.08	12	12	8	87.4
4	0.10	12	12	8	82.6
5	0.13	12	12	8	79.9
6	0.15	12	12	8	76.6
7	0.18	12	12	8	70.8
8	0.20	12	12	8	65.3
9	0.23	12	12	8	62.7
10	0.25	12	12	8	60.2
11	0.18	12	12	8	64.3
12	0.30	12	12	8	66.7

external magnetic induction intensity. More specifically, the maximum magnetic induction intensities are 1.07 T, 1.06 T, 1.03 T, and 0.97 T at external magnetic induction intensity values of 0.05 T, 0.1 T, 0.2 T, and 0.3 T, respectively. This fact is attributed to the workpiece that can be magnetized by the external magnetic field due to ferromagnetism. Besides, the magnetization phenomenon can also affect the electromagnetic induction phenomenon caused by the discharge current. Then, the maximum magnetic induction intensity of workpiece decreases along with the external magnetic flux density.

Figure 11 shows the stress distribution and corner deformation under the external magnetic field during single pulse discharge, and the scale factor of deformation is 1.12×10^7. It can be observed that (1) the maximum stress is obtained at the edge of the cutting kerf near wire electrode. This is inconsistent with the representation in Fig. 5. This fact is because the external magnetic field not only influences the magnetic field distribution but also applies a force on corner area. This force is actually the attractive force of the magnetic iron. (2) Figure 12 shows the influence trend of magnetic induction intensity on the maximum corner deformation. More specifically, the maximum corner deformations are 9.51×10^{-6} μm, 7.14×10^{-6} μm, 6.25×10^{-6} μm, and 8.93×10^{-6} μm when the external magnetic induction intensities are 0.05 T, 0.1 T, 0.2 T, and 0.3 T, respectively. In other words, the corner deformation firstly decreases and then increases along with the increasing of the external magnetic induction intensity. There is optimal external magnetic induction intensity between 0.2 and 0.3 T for acquiring the minimum corner deformation.

It can be concluded that the external magnetic field can effectively reduce the corner deformation through improving the magnetic field distribution. It should be noted though that this positive effect does not grow as the external magnetic

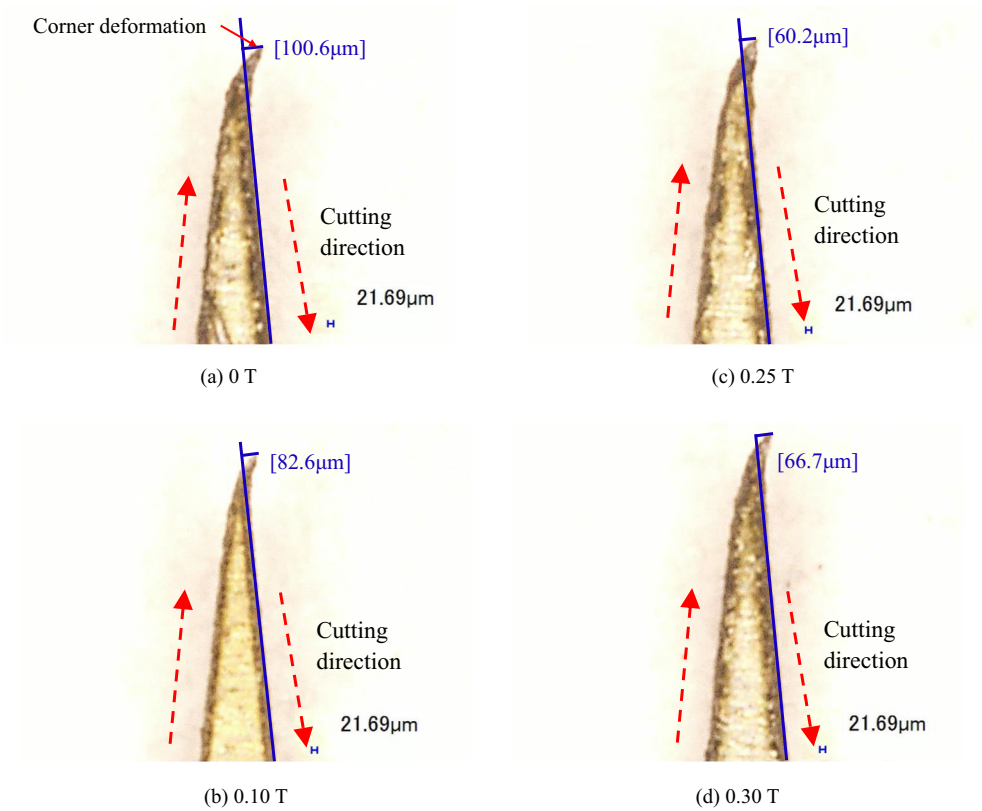

Fig. 15 The measurement drawing of corner deformation

Table 6 The input parameters and their levels of Taguchi experiment

Factors	Levels				
B (T)	0.10	0.15	0.20	0.25	0.30
t_{on} (μs)	8	10	12	14	16
t_{off} (μs)	8	10	12	14	16
I (A)	6	8	10	12	14

induction intensity rises. For revealing this phenomenon, the sharp-corner deformation under three machining conditions had been simulated, as shown in Fig. 13. When the external magnetic field is not applied, there is an attractive force (F_1) acting on the corner area caused by the induced magnetic field from discharge current, and its direction points to wire electrode. When the discharge current is zero, there is an attractive force (F_2) acting on the corner area caused by the external magnetic field, and its direction is in the same with the negative y-axis. These two attractive forces (F_1 and F_2) can all exacerbate the sharp-corner deformation. Increasing the external magnetic field intensity can reduce the maximum magnetic field intensity and the attractive force (F_1), but increase the attractive force (F_2). Then, the sharp-corner deformation may

Table 7 The results of Taguchi experiment

No.	B (T)	t_{on} (μs)	t_{off} (μs)	I (A)	D (μm)
1	0.1	8	8	6	62.5
2	0.1	10	10	8	68.9
3	0.1	12	12	10	77.8
4	0.1	14	14	12	89.8
5	0.1	16	16	14	97.6
6	0.15	8	10	10	62.7
7	0.15	10	12	12	67
8	0.15	12	14	14	79.4
9	0.15	14	16	6	62.1
10	0.15	16	8	8	83.3
11	0.2	8	12	14	59.1
12	0.2	10	14	6	52.3
13	0.2	12	16	8	58.1
14	0.2	14	8	10	72.7
15	0.2	16	10	12	77.1
16	0.25	8	14	8	41.1
17	0.25	10	16	10	51.2
18	0.25	12	8	12	68.8
19	0.25	14	10	14	74
20	0.25	16	12	6	58.1
21	0.3	8	16	12	50.7
22	0.3	10	8	14	70.7
23	0.3	12	10	6	52.6
24	0.3	14	12	8	64.5
25	0.3	16	14	10	65.6

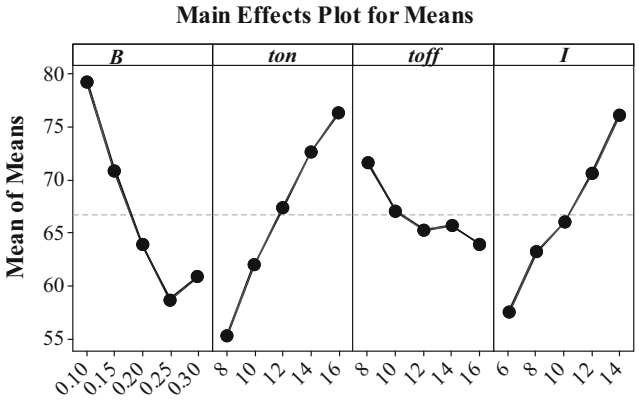

Fig. 16 The result of the main effect analysis of process parameters on the corner deformation

firstly decrease and then increase with the increasing of the external magnetic induction intensity.

Consequently, there is optimal external magnetic induction intensity for acquiring the minimum corner deformation. However, it should be pointed out that the optimal external magnetic induction intensity cannot be solved out by the coupled magnetic-mechanical model during single pulse discharge, and the reason of this fact is as follows: (a) The number of discharge spark is extremely high. (b) The distribution of discharge spark points is very complex and random. (c) There is interaction effect between numerous discharge sparks. Hence, this model can only qualitatively clarify the function mechanism of the external magnetic field on the corner deformation.

Summarizing, it is proved that the external magnetic field can effectively improve the magnetic field distribution and decrease the corner deformation. Besides, there is optimal external magnetic induction intensity for acquiring the minimum corner deformation.

3 Verification for the coupled model

In this section, an experimental study is implemented to verify the theoretical influence rule of the external magnetic field on the corner deformation.

All experiments are conducted on our self-developed 5-axis low-speed wire electrical discharge machine tool whose physical map is represented in Fig. 14. This machine tool mainly consists of wire winding system, pulse power source (in milliseconds), CNC system, workbench, 5-axis motion platform, cooling system, et al. The wire electrode is 0.25 mm in diameter brass wire; the dielectric is deionized water. Besides, the Keyence digital microscope (VH-Z500R) is used as a measuring tool in this experiment, and the magnification is × 200. Moreover, Q235 steel is chosen as the workpiece material because of its good magnetic conductivity. The chemical compositions and ranges of Q235 are shown in

Table 8 Response for main effect analysis

Level	B (T)	t_{on} (μs)	t_{off} (μs)	I (A)
1	79.32	55.22	71.6	57.52
2	70.9	62.02	67.06	63.18
3	63.86	67.34	65.3	66
4	58.64	72.62	65.64	70.68
5	60.82	76.34	63.94	76.16
Delta	20.68	21.12	7.66	18.64
Rank	2	1	4	3

Table 3. The physical and mechanical properties of Q235 are shown in Table 4.

Furthermore, according to our previous researches [12, 25] and experimental experience, four process parameters are selected as the variable factors, namely pulse on time (t_{on}), pulse-off time (t_{off}), discharge peak current (I), and the external magnetic induction intensity (B). Besides, other parameters are as shown in the following: gap voltage reference is 40 V, wire speed is 0.15 m/s, dielectric pressure is 1.0 MPa, wire tension is 15 N, corner cutting angle is 5°.

The design and results of the single factor experiment are listed in Table 5. Here, D represents corner deformation. Besides, Fig. 15 suggests the measurement drawing of corner deformation without and with the external magnetic field assisted.

From Table 5, it can be observed that (1) the external magnetic field can effectively reduce corner deformation. More specifically, the external magnetic field decreases the corner deformation from 100.6 to 60.2 μm. (2) Under constant other system parameters, the corner deformation decreases as the external magnetic induction intensity (B) increases up to the value of 0.25 T, followed by a rising path as the external magnetic induction intensity continues to increase. This observation is consistent with the influence as described by the coupled theoretical model. In other words, it is proved that the coupled magnetic-mechanical model is feasible and reliable.

4 The optimal process parameter combination for the minimum corner deformation

In this section, a group of Taguchi experiment is completed under the external magnetic-assisted approach for analyzing the influences of process parameters on the corner deformation and searching the optimal process parameter combination for the minimum corner deformation. The input parameters and their levels are listed in Table 6. The results of Taguchi experiment are indicated in Table 7.

The method of main effect analysis is adopted to evaluate the influences of process parameters on the corner deformation. Figure 16 shows the results of the main effect analysis of process parameters on the corner deformation, and Table 8 suggests the response for main effect analysis. It can be found in the following that:

a) With the increase of the external magnetic induction intensity, the corner deformation firstly rises and then drops down. This impact trend of the external magnetic induction intensity on the corner deformation corresponds with that in the single factor experiment.
b) The deltas of discharge parameters rank from high to low as follows: pulse-on time, external magnetic induction intensity, discharge peak current, and pulse-off time.

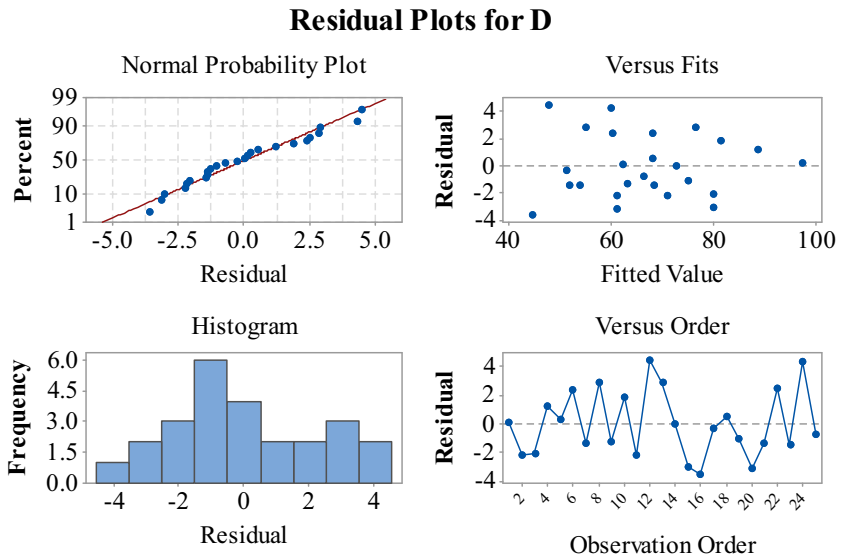

Fig. 17 The residual graphs for corner deformation

c) Corner deformation has a positive relation with discharge current. This fact can be explained by the coupled magnetic-mechanical model, the main reason of corner deformation is the induced magnetic field generated by discharge current, and the induced magnetic induction intensity rises with the increase of discharge peak current.
d) Corner deformation increases with the increase of pulse-on time. This fact is due to that the discharge energy of the single discharge pulse has positive correlation with pulse-on time. As we know, the removing mechanism of workpiece material in WEDM is always considered as thermal corrosion. So much high thermal energy density causes the workpiece material to melt or even vaporize [30, 31]. Thermal energy can not only remove workpiece material but it can also reduce the mechanical strength of the corner area material. In other words, increasing discharge current means decreasing the mechanical strength of the corner area material so as to increase the corner deformation.
e) Corner deformation reduces along with pulse-off time. On the one hand, the discharge energy of the single discharge pulse is inversely related to pulse-off time. On the other hand, the longer pulse-off time means the longer time for dielectric flushing without discharge spark. Then, the temperature of the corner area material can be fallen further. Namely, increasing pulse-off time can increase the mechanical strength of the corner area material in the discharge process.

Besides, the function of corner deformation in relation to the process parameters is established using nonlinear regression model, as shown in Eq. (2). The residual graphs for corner deformation are indicated in Fig. 17. It can be found that the fitting residual for corner deformation obeys normal distribution well. The average relative error between experimental data and fitting data is less than 3.1%. Moreover, the optimal machining parameter combination can be found out from the range analysis method, as follows: the external magnetic induction intensity is 0.25 T, pulse on time is 8 μs, pulse-off time is 16 μs, and discharge peak current is 6 A. According to the numerical model, the predicted value of corner deformation is at 38.5 μm.

$$D = 53.6315 - 284.84B + 657.71B^2 + 3.8071T_{on} - 0.9994 * T_{off} + 2.21I - 5.9BT_{on} - 0.597BI \quad (2)$$

Furthermore, a verified experiment is carried out to evaluate the precision of the numerical model for corner deformation, and to obtain the minimal corner deformation. Figure 18 suggests the measurement drawing of corner deformation under the optimal process parameter combination. It can be seen that the corner deformation is decreased to as small as 34.3 μm. The relative error between predicted value and experimental data is 4.2 μm, which suggests that the proposed numerical model has high precision. This error is composed of model error and measuring error. All data show that the magnetic-assisted methods with parameter optimization can effectively improve the corner accuracy in WEDM.

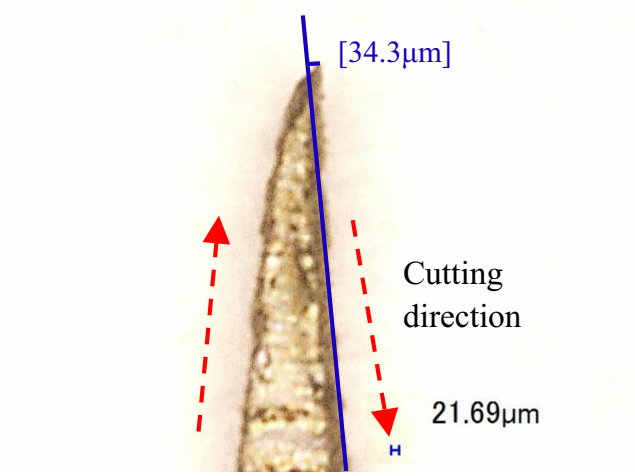

Fig. 18 The measurement drawing of corner deformation under the optimal process parameter combination

5 Conclusions

The main purpose of this study is to improve the corner accuracy of thin-walled sharp-corner part through magnetic field-assisted WEDM and parameter optimization. From the above analysis, the following conclusions can be drawn:

1. The coupled magnetic-mechanical model demonstrates that the external magnetic-assisted method can effectively improve the magnetic field distribution and decrease the corner deformation. Moreover, the corner deformation firstly decreases and then increases with the increase of the induction intensity of the external magnetic field. There is an optimal value of the external magnetic induction intensity for acquiring smaller corner deformation.
2. The single factor experiment indicates that the theoretical influence rule of the external magnetic field-assisted method on corner deformation is in good agreement with the experimental data. The maximal reduction of corner deformation reaches 40% when the external magnetic induction intensity is set as 0.25 T.
3. Taguchi experiment results clarify that the corner deformation rises up with the increase of pulse on time and discharge peak current, and reduces along with pulse-off time. Moreover, the numerical model of corner deformation depending on process parameters is obtained with high precision. Then, the optimal process parameter

combination is found out which can reduce corner deformation to as small as 34.3 μm.

Funding information This research is supported by National Natural Science Foundation of China (Grant No. 51805552), and the Project of State Key Laboratory of High Performance Complex Manufacturing, Central South University No. ZZYJKT2018-10.

References

1. Li ZL, Tuysuz O, Zhu LM, Altintas Y (2018) Surface form error prediction in five-axis flank milling of thin-walled parts. Int J Mach Tools Manuf 128:21–32
2. Wang D, Wu S, Bai Y, Lin H, Yang Y, Song C (2017) Characteristics of typical geometrical features shaped by selective laser melting. J Laser Appl 29(2):022007
3. Chen Z, Zhang Y, Zhang G, Huang Y, Liu C (2017) Theoretical and experimental study of magnetic-assisted finish cutting ferromagnetic material in wedm. Int J Mach Tools Manuf 123:36–47
4. Chen Z (2019) Study on the white layer in wire electrical discharge trim cutting of bearing steel GCr15. Int J Adv Manuf Technol 102(5–8):2375–2386
5. Chen Z, Zhang Y, Zhang G et al (2019) Investigation on a novel surface microstructure wire electrode for improving machining efficiency and surface quality in WEDM. Int J Adv Manuf Technol 102(5–8):2409–2421
6. Han F, Zhang J, Soichiro I (2007) Corner error simulation of rough cutting in wire EDM. Precis Eng 31(4):331–336
7. Chen Z, Huang Y, Zhang Z, Li H, Ming WY, Zhang G (2014) An analysis and optimization of the geometrical inaccuracy in WEDM rough corner cutting. Int J Adv Manuf Technol 74(5–8):917–929
8. Abyar H, Abdullah A, Akbarzadeh A (2018) Analyzing wire deflection errors of WEDM process on small arced corners. J Manuf Process 36:216–223
9. Chen Z, Zhang Y, Zhang G (2018) Modeling and reducing workpiece corner error due to wire deflection in WEDM rough corner-cutting. J Manuf Process 36:557–564
10. Chen Z, Zhang G, Yan H (2018) A high-precision constant wire tension control system for improving workpiece surface quality and geometric accuracy in WEDM. Precis Eng 54:51–59
11. Tomura S, Kunieda M (2009) Analysis of electromagnetic force in wire-EDM. Precis Eng 33(3):255–262
12. Chen Z, Huang Y, Huang H, Zhang Z, Zhang G (2015) Three-dimensional characteristics analysis of the wire-tool vibration considering spatial temperature field and electromagnetic field in WEDM. Int J Mach Tools Manuf 92:85–96
13. Nani VM (2016) The ultrasound effect on technological parameters for increase in performances of W-EDM machines. Int J Adv Manuf Technol 88(1–4):1–10
14. Gholipoor A, Baseri H, Shakeri M, Shabgard M (2014) Investigation of the effects of magnetic field on near-dry electrical discharge machining performance. Proc Inst Mech Eng Part B-J Eng Manuf 230(4)
15. Lin YC, Lee HS (2008) Machining characteristics of magnetic force-assisted EDM. Int J Mach Tools Manuf 48(11):1179–1186
16. Lin YC, Chen YF, Wang DA, Lee HS (2009) Optimization of machining parameters in magnetic force assisted EDM based on Taguchi method. J Mater Process Technol 209(7):3374–3383
17. Lin YC, Chuang FP, Wang AC, Chow HM (2014) Machining characteristics of hybrid EDM with ultrasonic vibration and assisted magnetic force. Int J Precis Eng Manuf 15(6):1143–1149
18. Teimouri R, Baseri H (2014) Optimization of magnetic field assisted EDM using the continuous aco algorithm. Appl Soft Comput 14(1):381–389
19. Govindan P, Gupta A, Joshi SS, Malshe A, Rajurkar KP (2013) Single-spark analysis of removal phenomenon in magnetic field assisted dry EDM. J Mater Process Technol 213(7):1048–1058
20. Teimouri R, Baseri H (2012) Effects of magnetic field and rotary tool on EDM performance. J Manuf Process 14(3):316–322
21. Teimouri R, Baseri H (2013) Experimental study of rotary magnetic field-assisted dry EDM with ultrasonic vibration of workpiece. Int J Adv Manuf Technol 67(5–8):1371–1384
22. Heinz K, Kapoor SG, Devor RE, & SurlaV (2015). An investigation of magnetic-field-assisted material removal in micro-EDM for nonmagnetic materials. J Manuf Sci Eng 133(2):021002
23. Ming W, Zhang Z, Wang S et al (2019) Comparative study of energy efficiency and environmental impact in magnetic field assisted and conventional electrical discharge machining. J Clean Prod 214:12–28
24. Zhang Y, Zhang Z, Zhang G, Li W (2019) Reduction of energy consumption and thermal deformation in WEDM by magnetic field assisted technology. Int J Pr Eng Man-GT:1–14. https://doi.org/10.1007/s40684-019-00086-5
25. Zhang Z, Huang H, Ming W, Xu Z, Huang Y, Zhang G (2016) Study on machining characteristics of WEDM with ultrasonic vibration and magnetic field assisted techniques. J Mater Process Technol 234:342–352
26. Wang Y, Wang Q, Ding Z, He D, Xiong W, Chen S et al (2018) Study on the mechanism and key technique of ultrasonic vibration and magnetic field complex assisted WEDM-LS thick shape memory alloy workpiece. J Mater Process Technol 261:202–212
27. Chen Z, Yan Z, Yan H et al (2019) Improvement of the machining characteristics in WEDM based on specific discharge energy and magnetic field-assisted method. Int J Adv Manuf Technol 103(5–8):3033–3044
28. Wang K, Zhang Q, Zhu G, Liu Q, Huang Y, Zhang J (2017) Research on the energy distribution of micro EDM by utilization of electro-thermal model. Int J Adv Manuf Technol 93(5–8):1–8
29. Hoang KT, Gopalan SK, Yang SH (2015) Study of energy distribution to electrodes in a micro-EDM process by utilizing the electro-thermal model of single discharges. J Mech Sci Technol 29(1):349–356
30. Han F, Cheng G, Feng Z, Isago S (2008) Thermo-mechanical analysis and optimal tension control of micro wire electrode. Int J Mach Tools Manuf 48(7):922–931
31. Cheng G, Han F, Feng Z (2007) Experimental determination of convective heat transfer coefficient in WEDM. Int J Mach Tools Manuf 47(11):1744–1751